Available online at www.sciencedirect.com
ScienceDirect
Organic Electronics 9 (2008) 101–110
Organic Electronics
www.elsevier.com/locate/orgel

Iminodibenzyl-substituted distyrylarylenes as dopants for blue and white organic light-emitting devices

Meng-Huan Ho [a,*], Chia-Ming Chang [a], Ta-Ya Chu [b], Teng-Ming Chen [a], Chin H. Chen [c]

[a] Department of Applied Chemistry, National Chiao Tung University, Hsinchu 300, Taiwan, ROC
[b] Department of Electrophysics, National Chiao Tung University, Hsinchu 300, Taiwan, ROC
[c] Display Institute, Microelectronics and Information Systems Research Center, National Chiao Tung University, Hsinchu 300, Taiwan, ROC

Received 21 March 2007; received in revised form 9 July 2007; accepted 28 September 2007
Available online 9 October 2007

Abstract

A series of highly efficient blue materials based on iminodibenzyl-substituted distyrylarylene (IDB-series) fluorescent dyes using the concept of steric-compression have been designed and synthesized by means of a rigidized and over-sized ring. The steric-compression effect can shorten the effective conjugation length (chromophore) of the molecule and the added phenyl moiety in the core can alleviate the propensity for molecular aggregation. These materials also possess high glass transition temperature over 100 °C. The blue IDB-Ph device achieved a maximum external quantum efficiency of 4.8% with a Commission Internationale de l'Eclairage ($CIE_{x,y}$) coordinate of (0.16, 0.28). When applied in two-element white OLED system, the IDB-Ph doped device achieved a luminance efficiency of 11.0 cd/A with a $CIE_{x,y}$ color coordinate of (0.29, 0.36).

PACS: 78.55.Kz; 78.60.Fi; 85.60.Jb

Keywords: Iminodibenzyl; Distyrylarylenes; Fluorescent blue material; Organic electroluminescent device

1. Introduction

Recently, owing to their unique electrical and optical properties, various functional devices using organic materials have been developed in a variety of applied fields [1]. Since the initial work by Tang and Van Slyke [2], interest in organic light-emitting diodes (OLEDs) has been steadily growing. In particular, OLEDs have been the subject of intensive investigation because of their successful commercialization in various full-color displays [3,4]. Materials development continues to play a pivotal role in this technology as OLED materials have to function often not only as a charge transporter but also an efficient light emitter. Morphology stability of various layers is another issue that needs to be addressed to assure sufficient long operational lifetime for the devices [5,6].

To date, white organic light-emitting devices (WOLEDs) have drawn intensive studies due to their potential applications in full-color display

* Corresponding author.
E-mail address: kinneas.ac94g@nctu.edu.tw (M.-H. Ho).

1566-1199/$ - see front matter
doi:10.1016/j.orgel.2007.09.006

fabrication with color filters [7], in backlight for liquid crystal display as well as in solid-state lightings [8]. One of the best known methods to achieve WOLEDs is the two-color system of sky blue and yellow or orange emission, which has been widely reported [9–11]. In this system, it has been shown that performance of WOLEDs can be improved significantly by adopting sky blue fluorescent materials with high efficiency, optimized color, and long operational stability. To this end, there have been a number of efficient blue fluorescent dyes developed in the past several years [12–15], especially the di(styryl)- amine-based blue dopant, DSA-Ph [16] and BUBD-1 [17] which, upon doping in the morphologically stable host material, 2-methyl-9,10-di(2-naphthyl)anthracene (MADN), their device performances achieved an EL efficiency of 9.7 cd/A with $CIE_{x,y}$ of (0.16, 0.32) and 13.2 cd/A with $CIE_{x,y}$ of (0.16, 0.30) at 20 mA/cm^2, respectively.

In this paper, we disclose a newly designed series blue dopants based on the 7-membered *N*-heterocyclic core structure of iminodibenzyl-distyrylarylene (IDB). It has been reported that when general aromatic amino-substituents (e.g. diphenyl amine) of hole transport material are replaced with the *iminodibenzyl* groups, the thermal properties can be improved and the emission wavelength would be blue-shifted [18,19]. Hence, we decided to introduce the iminodibenzyl groups into the highly fluorescent distyrylarylene structure. From *ab initio* density functional theory (DFT) using B3LYP/6-31* level of basis sets, we also found that the emission wavelength could be shifted to slightly deeper blue with increasing the number of phenyl moiety in the center core. We expect these new blue materials will be potentially useful in producing a deep blue emission with a properly matched host and a two-element white OLED system as well.

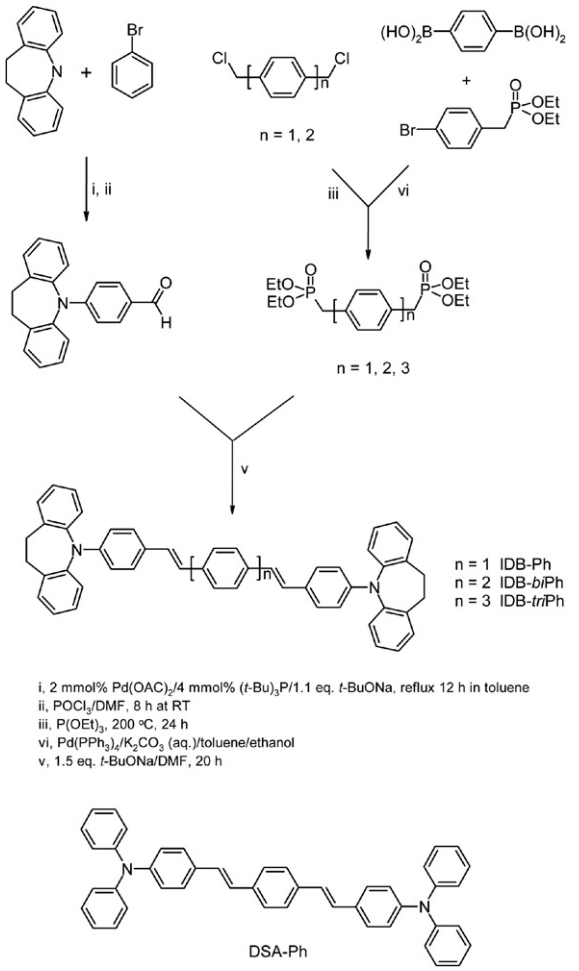

Scheme 1. Synthetic routes of IDB-series materials and structure of DSA-Ph.

2. Experimental

2.1. Synthesis

The synthetic routes of iminodibenzyl-substituted distyrylarylene derivatives (IDB-series) are shown in Scheme 1. The intermediate 4-(iminodibenzyl)-benzoaldehyde was prepared by coupling iminodibenzyl (IDB) and 4-bromobenzene with a palladium-catalyzed aromatic amination reaction [20]. After the reaction was completed, 9-phenyl-iminodibenzyl was purified by column chromatography and then mixed with phosphoryl chloride in DMF at room temperature for 8 h under nitrogen [21]. The mixture was quenched with sodium acetate and water to precipitate the gray solid and purified by recrystallization twice from ethanol to afford the intermediate as colorless crystal.

On the other hand, a mixture of *p*-xylylene dichloride and neat triethyl phosphite was heated at 200 °C for 24 h under nitrogen. After cooling to room temperature, the reaction mixture was purified by bulb to bulb distillation to afford tetraethyl *p*-(xylylene)diphosphonate [22]. The tetraethyl biphenyl-4,4′-diylbis(methylene)diphosphonate was synthesized from 4,4′-bis(chloromethyl)-biphenyl with same procedure. The tetraethyl triphenyl-4,4″-diybis(methylene)diphosphonate was synthesized by adding aqueous K_2CO_3 (2.0 M, 20 mL) to

a solution of diethyl-4-bromobenzyl phosphonate (4.5 mmol) and 1,4-benzenediboronic acid (1.9 mmol) in toluene (60 mL) and ethanol (10 mL). The mixture was degassed and tetrakis(triphenylphosphine) palladium (3.9 mol%) was added in one portion under an atmosphere of N_2 and then heated under reflux for 24 h [23]. After the solution cooled, the solvent was evaporated under vacuum and the product was extracted with ethyl acetate. The organic solution was washed with water several times and dried with anhydrous $MgSO_4$, followed by recrystallization from ethanol.

Finally, the IDB-series materials were readily synthesized by Horner–Wadsworth–Emmons reaction according to a known procedure [24]. To a solution of 4-(iminodibenzyl)-benzoaldehyde (2.1 mmol) and the appropriate phosphonate (1 mmol) in DMF cooled in an ice bath, sodium *tert*-butoxide (1.5 mmol) was added and stirred at 25 °C for 20 h. The mixture was then poured into water, and the precipitated product was collected and washed with methanol. The crude product was purified by chromatography to give pure IDB-series material as a yellow solid. The final products were purified by temperature gradient sublimation before using in subsequent studies.

tetraethyl *p*-(xylylene)diphosphonate. ^{1}H NMR (300 MHz, $CDCl_3$): δ/ppm 1.19 (t, 12H), 3.08 (d, 4H), 3.99-4.03 (m, 8H), 7.23 (s, 4H).

tetraethyl biphenyl-4,4′-diylbis(methylene)diphosphonate. ^{1}H NMR (300 MHz, $CDCl_3$): δ/ppm 1.22 (t, 12 H), 3.14 (d, 4H), 4.00–4.04 (m, 8H), 7.35 (d, 4H), 7.51 (d, 4H).

tetraethyl biphenyl-4,4″-diylbis(methylene)diphosphonate. ^{1}H NMR (300 MHz, $CDCl_3$): δ/ppm 1.24 (t, 12H), 3.19 (d, 4H), 4.03–4.08 (m, 8H), 7.23–7.64 (m, 12H).

IDB-Ph. ^{1}H NMR (300 MHz, $CDCl_3$): δ/ppm 3.00 (s, 8H), 6.56 (d, 4H), 6.82–6.97 (m, 4H), 7.21–7.43 (m, 24H). FAB-MS: $m/z = 668$ (M^+). Anal. for $C_{50}H_{40}N_2$: Calcd: C, 89.78; H, 6.03; N, 4.19. Found: C, 89.14; H, 5.83; N, 3.66.

IDB-biPh. ^{1}H NMR (300 MHz, $CDCl_3$): δ/ppm 3.00 (s, 8H), 6.59 (d, 4H), 6.89–7.08 (m, 8H), 7.23–7.60 (m, 24H). FAB-MS: $m/z = 744$ (M^+). Anal. for $C_{56}H_{44}N_2$: Calcd: C, 90.29; H, 5.95; N, 3.76. Found: C, 89.72; H, 5.82; N, 3.46.

IDB-triPh. ^{1}H NMR (300 MHz, $CDCl_3$): δ/ppm 3.00 (s, 8H), 6.56(d, 4H), 6.87–7.06 (m, 8H), 7.20–7.66 (m, 28H). FAB-MS: $m/z = 820$ (M^+). Anal. for $C_{62}H_{48}N_2$: Calcd: C, 90.70; H, 5.89; N, 3.41. Found: C, 89.91; H, 5.83; N, 2.95.

2.2. Characterization of material properties

All IDB-series materials were further purified via train sublimation and fully characterized with satisfactory spectroscopic data. UV–Vis and solution photoluminescence spectra were recorded in toluene by Hewlett Packard 8453 and Acton Research Spectra Pro-150, respectively. Electrochemical properties were studied by cyclic voltammetry using CHI 604 A. The energy gap can be calculated from the edge of UV–Vis absorption peak. Melting points (T_m), Glass transition temperatures (T_g) of the respective compounds were measured by differential scanning calorimetry (DSC) under nitrogen atmosphere using a SEIKO SSC 5200 DSC Computer/thermal analyzer.

2.3. Geometry optimization

The ground-state structures of IDB-series materials were optimized by using *ab initio* density functional theory (DFT) with the B3LYP (Becke three-parameter Lee–Yang–Parr) [25,26] exchange correlation function with 6-31G* basis sets, in Gaussian 03 program [27].

2.4. Device fabrication

The structures of blue and white devices and materials applied in this study are shown in Fig. 1. In the device fabrication, CF_x, *N*,*N*′-bis-(1-naphthyl)-*N*,*N*′-diphenyl,1,1′-biphenyl-4,4′-diamine (NPB), *tris*(8-quinolinolato)aluminium (Alq_3), and LiF were used as hole injection [28], hole transport, electron transport and electron injection materials, respectively. The emitting layer (EML) of blue-doped devices is composed of blue IDB dopants doped in the stable blue host material of MADN with each optimized concentration. In two-element WOLED device, the sky-blue light emission was generated by doping 7% highly fluorescent IDB-Ph into MADN while the yellow emission was derived from the doping 4% 2,8-di(*t*-butyl)-5,11-di [4-(*t*-butyl)phenyl]-6,12-diphenylnaphthacene (TBRb) [29] in NPB to obtain a white emission.

After a routine cleaning procedure, the indium-tin-oxide (ITO)-coated glass was loaded on the grounded electrode of a parallel-plate plasma reactor, pretreated by oxygen plasma, and then coated with a polymerized fluorocarbon film. Devices were fabricated under the base vacuum of about 10^{-6} torr in a thin-film evaporation coater following

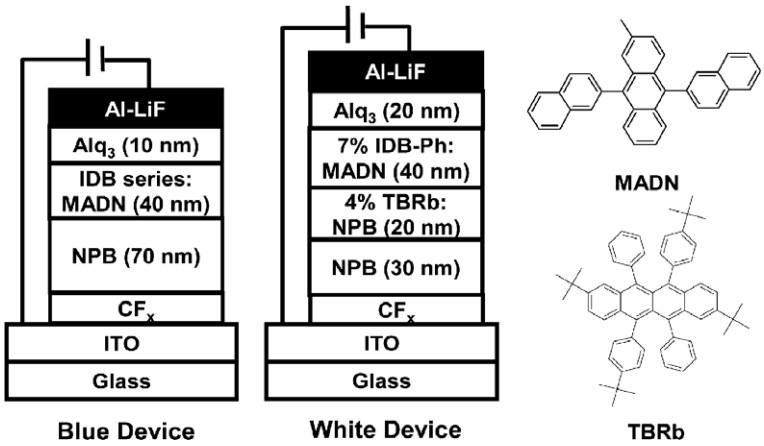

Fig. 1. Structures of MADN, TBRb, blue and white devices.

a published protocol [30]. In the evaporation of EML, the fluorescent dopant was co-deposited with host molecule at its optimal molar ratio. After the thermal deposition of the organic layers and without a vacuum break, the ultra thin layer of 1 nm of LiF followed by 200 nm of Al was deposited through a patterned shadow mask on top of the organic layers using separately controlled sources to complete the cathode. All devices were hermetically sealed prior to testing. The active area of the EL device, defined by the overlap of the ITO and the cathode electrodes, was 9 mm^2. The current–voltage–luminance characteristics of the devices were measured with a diode array rapid scan system using a Photo Research PR650 spectrophotometer and a computer-controlled programmable dc source. The device lifetime measurements were performed in a glove box at a constant drive current density of 20 mA/cm^2.

3. Results and discussion

3.1. Luminescence in solution

The photo-physical, electrochemical and thermal properties of DSA-Ph and IDB-series materials are summarized in Table 1. Fig. 2 compares the absorption and photoluminescence (PL) spectra of DSA-Ph and IDB-series materials in toluene. The features of the lowest absorption band and fluorescence of IDB-Ph are very similar to those of DSA-Ph, except they are blue-shifted. The emission wavelength of IDB-Ph is 449 nm which is blue-shifted around 9 nm with respect to that of DSA-Ph. From the conformational structures of DSA-Ph and IDB-Ph optimized by the density functional theory method using B3LYP/6-31* level of basis sets shown in Fig. 3, we found that the orthogonality between the distyrylarylene core and the phenyl group of iminodibenzyl substituent is higher than that between the core and phenyl group of diphenylamine substituent in the ground state. We attributed that the phenomenon is due to the rigid iminodibenzyl substituent which would increase the steric strain and cause the iminodibenzyl moiety to twist slightly out of the plane defined by the π–π conjugation of the distyrylarylene core. For example, the angle between the stilbene core and the phenyl group of iminodibenzyl (66°) is higher than that between the core and phenyl group of diphenylamine (42°). As a result, the effect of steric-compression would be the reason for the

Table 1
The photo-physical, electrochemical and thermal properties of DSA-Ph, IDB-Ph, IDB-biPh and IDB-triPh

Material	$\lambda_{abs,max}$ (nm)	$\lambda_{em,max}$ (nm)	HOMO (eV)	LUMO (eV)	Band gap (eV)	T_g (°C)	T_m (°C)
DSA-Ph	410	458	5.4	2.7	2.7	89	172
IDB-Ph	408	449	5.2	2.4	2.75	119	325
IDB-biPh	402	447	5.2	2.4	2.75	131	335
IDB-triPh	398	443	5.1	2.3	2.8	137	344

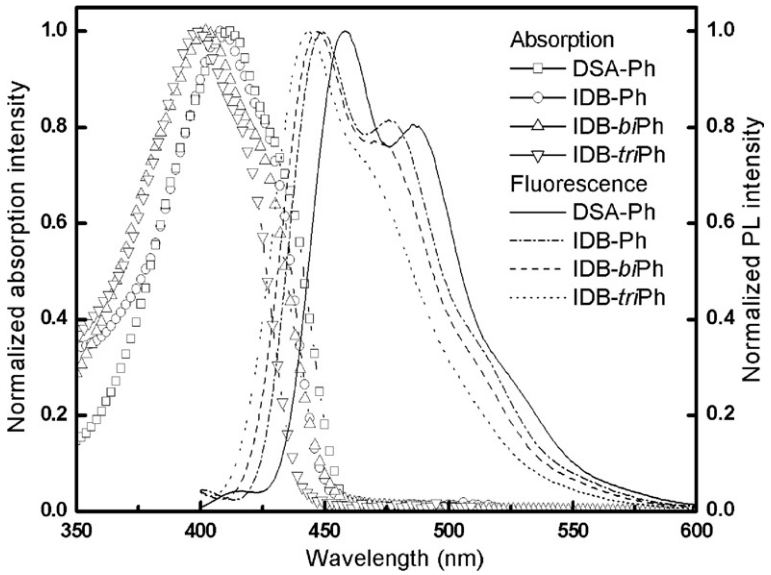

Fig. 2. Normalized absorption, photoluminescence (PL) spectra of DSA-Ph and IDB-series materials.

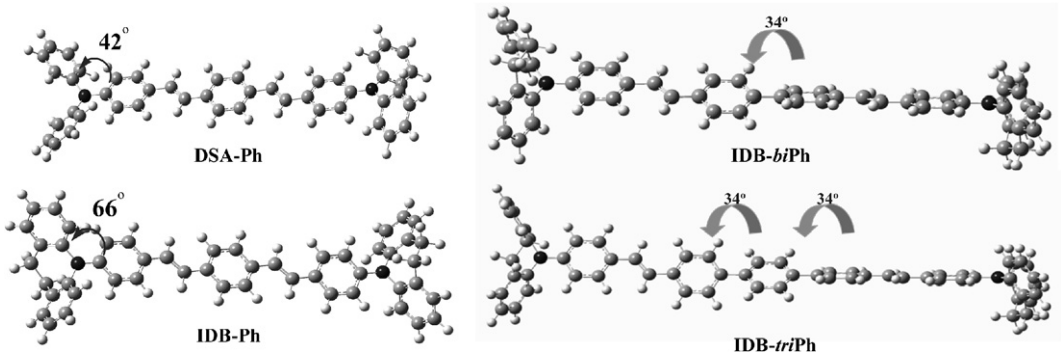

Fig. 3. Conformational Structures of DSA-Ph and IDB-series materials [DFT with B3LYP/6-31G(d)].

hypsochromic-shifted emission wavelength of IDB-Ph as compared to DSA-Ph.

It was also found that IDB-biPh and IDB-triPh (with emission λ_{max} 447 nm and 443 nm, respectively) have a slightly blue-shifted emission wavelength with respect to IDB-Ph, which means the optical spectra can be slightly shifted to shorter wavelength with the increasing phenyl moiety in the molecular core. This *hypsochromic*-shifted phenomenon can also be rationalized from the conformational structures of IDB-series materials shown in Fig. 3, in which the added phenyl moiety appears to enlarge the twist angle between two (styryl)iminodibenzyl chromophores and further decrease the π–π conjugation. As a result, the effective conjugation length (chromophore) of the molecule is slightly shortened and causes the emission wavelength to deeper blue region.

3.2. Luminescence in the solid state

In order to investigate the energy-transfer between host material (MADN) and dopant (IDB-series materials), we measured the solid-state emission spectra of various doping concentration of IDB materials doped in MADN thin films (excited with 400 nm, $\lambda_{ex,max}$ of MADN). As shown in Fig. 4a, the IDB-Ph emission can be clearly observed at 5% doping concentration and the emission of MADN around 430 nm essentially quenched confirming that the Förster energy-transfer from MADN to IDB-Ph is efficient. Moreover, when

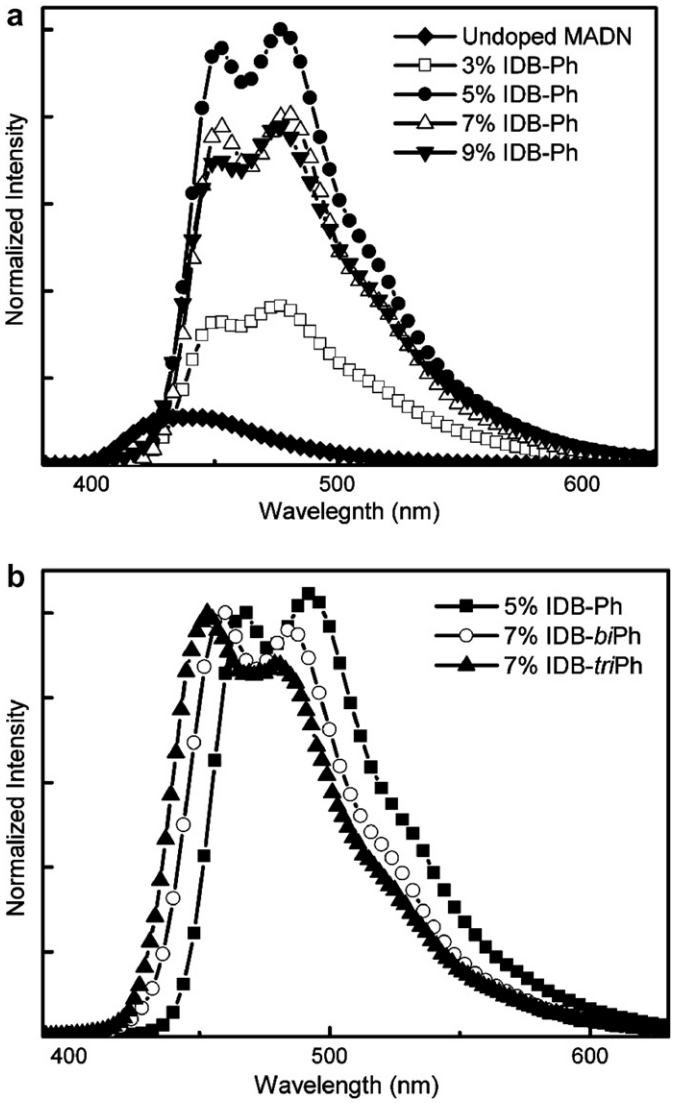

Fig. 4. (a) Solid state emission spectra of IDB-Ph/MADN thin films. (b) Normalized solid state emission spectra of IDB-series/MADN thin films.

doping concentration is up to 7%, the IDB-Ph emission intensity would be decreased and the intensity of long wavelength shoulder tends to grow with increasing doping concentration and appears to be even higher than that of the main peak. This phenomenon is primarily due to the molecular aggregation propensity of IDB-Ph with the flat stilbene-based center core, especially at high doping concentration.

The emission spectra of IDB-biPh/MADN and IDB-triPh/MADN thin films reveal the same results as there are also efficient Förster energy-transfer between IDB-biPh/MADN and IDB-triPh/MADN, respectively. Fig. 4b depicts the normalized solid-state emission spectra of IDB-series materials/MADN thin films. The solid-state emission spectra were similar to those recorded in toluene solution shown in Fig. 2. It is observed that the solid-state emission spectra become broader and the intensity of long wavelength shoulder become higher when compared with the solution PL spectra. Interestingly, the intensity of long wavelength shoulder and the full width at half maximum (FWHM) of solid-state emission spectra can be decreased with the increasing phenyl moiety in the molecular core. (The FWHM of solid-state emission of IDB-series

materials are $1.32 \times 10^5\ cm^{-1}$, $1.43 \times 10^5\ cm^{-1}$, $1.47 \times 10^5\ cm^{-1}$, respectively.) It was also found that the optimal doping concentration of IDB-biPh and IDB-triPh is 7% which is higher than that of IDB-Ph. Based on these results, we conclude that the introduction of added phenyl moiety can enlarge the twist angle in the center core and thus can alleviate the propensity for molecular aggregation. Therefore, the added phenyl moiety in the center core can be expected to further improve the color purity of blue-doped devices.

3.3. Electrochemical and thermal properties

The HOMO energy level of each material can be obtained by cyclic voltammetry and the energy-gap can be calculated from the edge of UV–Vis absorption peak. The measured HOMO energy levels of IDB-series materials are about 5.1–5.2 eV and are smaller than that of DSA-Ph (5.4 eV). This phenomenon can be rationalized by the strong donor characteristic of iminodibenzyl group, which has a small ionization potential (I_p) [31] and oxidation potential [32] and consequently causes the LUMO energy level of IDB-series dopants are much decreased to 2.3–2.4 eV.

We used differential scanning calorimetry (DSC) to investigate the thermal properties of IDB-series materials. The thermal characteristics of IDB-series materials are also summarized in Table 1. The glass transition temperature (T_g) of IDB-Ph, IDB-biPh and IDB-triPh are found at 119 °C, 131 °C and 137 °C, respectively, which are all much higher than that of DSA-Ph (89 °C). This result indicates that the steric iminodibenzyl substituent and the added phenyl moiety would not only affect the emission wavelength but also improve the material thermal stability. As a result, these IDB-series materials can form amorphous thin films that are more stable than that of DSA-Ph, and they are more promising in terms of their thermal stability for application in OLEDs.

3.4. Blue device performance

The EL efficiency of the undoped MADN is 1.5 cd/A at 20 mA/cm^2 with a $CIE_{x,y}$ color coordinate of (0.15, 0.10). When doped with IDB-Ph, IDB-biPh and IDB-triPh at their optimal doping concentrations of 5%, 7% and 7%, the EL efficiencies are increased to 9.1, 6.3, and 3.7 cd/A with $CIE_{x,y}$ color coordinate of (0.16, 0.28), (0.15, 0.24) and (0.13, 0.20), respectively. Their optimal doping levels are consistent with those of their corresponding solid-state thin film fluorescence yield. The overall EL performances of the new blue dopants doped devices are summarized in Table 2. The device performance indicates that the IDB-series materials are useful in producing blue OLED devices with high efficiency. The maximum external quantum efficiency (EQE) of IDB-Ph doped device is close to the theoretical limit of 4.8% and the half-decay lifetime ($t_{1/2}$) is 700 h with an initial brightness of 1976 cd/m^2 monitored in a dry box. Assuming the scalable law of Coulombic degradation [29] for driving at L_0 of 100 cd/m^2, the half-decay lifetime ($t_{1/2}$) of the IDB-Ph doped device is projected to be over 13,000 h.

Fig. 5 shows the normalized EL spectra of these blue-doped devices. The EL spectra peak and FWHM of dopants IDB-Ph, IDB-biPh and IDB-*tri*Ph are 461 nm, 460 nm, 456 nm and $1.39 \times 10^5\ cm^{-1}$, $1.47 \times 10^5\ cm^{-1}$, $1.67 \times 10^5\ cm^{-1}$, respectively, that are in good agreement with their corresponding solid-state emission spectra. Most importantly, the intensity of long wavelength shoulder is indeed suppressed with the increasing number of phenyl moiety at the molecular core which further improves the CIE y value to deeper blue (from 0.28 to 0.20).

3.5. Two-element white OLED device performance

We also introduced the new sky-blue emitter, IDB-Ph, into the white OLED structure incorporating a dual-layered emitting layer (EML) of blue and yellow to compose the white emission additively. Within the device structure, NPB doped with TBRb was used as the yellow emission layer. The performances of IDB-Ph doped WOLED are summarized

Table 2
Performance of IDB-series doped blue devices and two-element WOLED devices at 20 mA/cm^2

Blue dopant	Voltage (V)	Yied (cd/A)	Pow. Eff. (lm/W)	EQE (%)	$CIE_{x,y}$
Blue device					
IDB-Ph	5.9	9.1	4.9	4.8	(0.16, 0.28)
IDB-biPh	5.9	6.3	3.3	3.7	(0.15, 0.24)
IDB-triPh	6.8	3.7	1.7	2.5	(0.13, 0.20)
Two-element WOLEDs					
IDB-Ph	6.5	11.0	5.3	4.8	(0.29, 0.36)

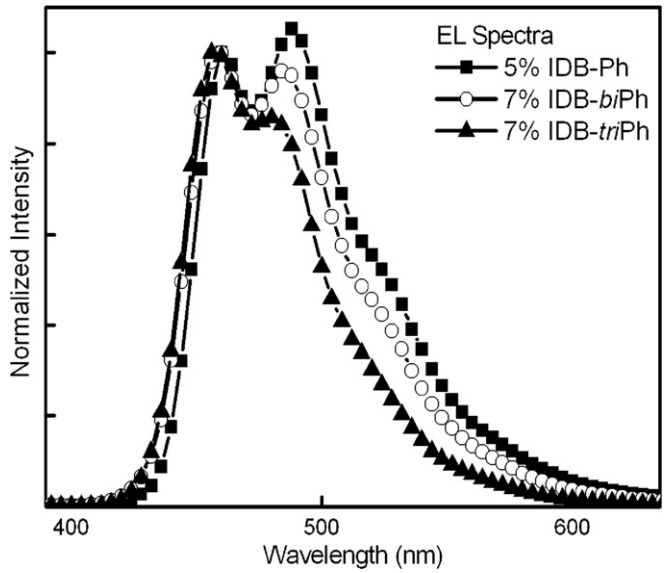

Fig. 5. Normalized EL spectra of IDB-series doped blue devices at 20 mA/cm^2.

in Table 2. The IDB-Ph doped WOLED can achieve an EL efficiency of 11.0 cd/A and 5.3 lm/W with a $CIE_{x,y}$ color coordinate of (0.29, 0.36) which are all better than the reported DSA-Ph doped WOLED [11]. The inset of Fig. 6 shows the EL spectra of IDB-Ph deoped WOLED, it covers a wild range of visible region, clearly indicating the emissions of IDB-Ph and TBRb with a dominant peak at 464, 488, and 564 nm, respectively. It is evident that there is no obvious EL color shift with increased driving currents from 20 mA/cm^2 to 200 mA/cm^2. Fig. 6 shows the operational lifetime of the IDB-Ph doped WOLED under a constant current density of 20 mA/m^2 monitored in a dry box. The t_{80} (the time for the luminance to drop to 80% of initial luminance) and initial luminance (L_0) is 420 h with an initial brightness of 2198 cd/m^2 monitored in a dry box. Assuming the scalable law of Coulombic degradation [29] for driving at L_0 of 100 cd/m^2, the half-decay lifetime ($t_{1/2}$) of

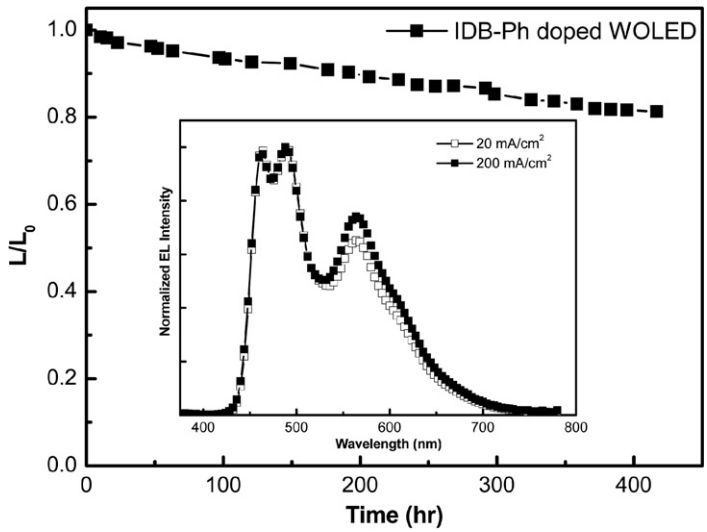

Fig. 6. Device operational stability of the IDB-Ph doped WOLED. Inset: The normalized EL spectra of IDB-Ph doped WOLED at various current densities.

the IDB-Ph doped device is projected to be over 42,000 h.

These results indicate that the two-element WOLED performance can really be significantly enahnced both in device efficiency and $CIE_{x,y}$ color coordinates by replacing DSA-Ph to IDB-Ph. The improved result is due to the new blue emitter, IDB-Ph, which emits deeper blue light with higher efficiency and better thermal stability than that of DSA-Ph. Therefore, when this new blue emitter was used in a two-element WOLED system, it can achieve a high EQE of 4.8% and generate a more balanced white $CIE_{x,y}$ color coordinates.

4. Conclusions

By molecular engineering of the di(styryl)amine-based structure, we have designed and synthesized a series of highly efficient blue dopants based on the iminodibenzyl-substituted distyrylarylene (IDB-series) compounds. The steric-compression effect can shorten the effective conjugation length (chromophore) of the molecule and the added phenyl moiety in the core can alleviate the propensity for molecular aggregation. These materials also possess high glass transition temperature over 100 °C. When doped in the stable blue host material, MADN, the maximum external quantum efficiency of IDB-Ph doped device is close to the theoretical limit of 4.8% with a $CIE_{x,y}$ color coordinate of $(0.16, 0.28)$. When IDB-Ph was used in a two-element WOLED system, the doped device achieved a luminance efficiency of 11.0 cd/A at 20 mA/cm^2 with a $CIE_{x,y}$ color coordinate of $(0.29, 0.36)$. The white device achieved a half-decay lifetime ($t_{1/2}$) of 42,000 h at an initial brightness of 100 cd/m^2.

Acknowledgements

This work was supported by grants from Chunghwa Picture Tubes, Ltd. (CPT) of Taoyuan, Taiwan. and National Science Council of Taiwan. We thank e-Ray Optoelectronics Technology Co., Ltd. of Taiwan for generously supplying some of the OLED materials studied in this work.

References

[1] M. Pope, C. Swenberg, Electronic Processes in Organic Crystals and Polymers, Oxford Science Publcations, New York, 1999.
[2] C.W. Tang, S.A. Van Slyke, Appl. Phys. Lett. 51 (1987) 913.
[3] U. Mitschke, P. Bauerle, J. Mater. Chem. 10 (2000) 1471.
[4] L.S. Hung, C.H. Chen, Mater. Sci. Eng. R 39 (2002) 143.
[5] S. Tokido, H. Tanaka, K. Noda, A. Okada, T. Taga, Appl. Phys. Lett. 70 (1997) 1929.
[6] P. Fenter, F. Schreiber, V. Buloviæ, S.R. Forrest, Chem. Phys. Lett. 277 (1997) 521.
[7] J. Kido, K. Nagai, K. Okutama, Appl. Phys. Lett. 64 (1994) 815.
[8] Y. Sun, N.C. Giebink, H. Kanno, B. Ma, M.E. Thompson, S.R. Forrest, Nature 440 (2006) 908.
[9] M. Li, W.L. Li, J.H. Niu, B. Chu, B. Li, X.Y. Sun, Z.Q. Zhang, Z.Z. Hu, Solid-State Electron. 49 (2005) 1956.
[10] D. Gupta, M. Katiyar, Opt. Mater. 28 (2006) 295.
[11] Y.S. Wu, S.W. Hwang, H.H. Chen, M.T. Lee, W.J. Shen, C.H. Chen, Thin Solid Film 488 (2005) 265.
[12] W.J. Shen, R. Dodda, C.C. Wu, F.I. Wu, T.H. Liu, H.H. Chen, C.H. Chen, C.F. Shu, Chem. Mater. 16 (2004) 930.
[13] S. Tao, Z. Peng, X. Zhang, P. Wang, C.S. Lee, S.T. Lee, Adv. Funct. Mater. 15 (2005) 1716.
[14] Y.H. Kim, H.C. Jeong, S.H. Kim, K. Yang, S.K. Kwon, Adv. Funct. Mater. 15 (2005) 1799.
[15] B.K. Shah, D.C. Neckers, J. Shi, E.W. Forsythe, D. Morton, Chem. Mater. 18 (2006) 603.
[16] M.T. Lee, H.H. Chen, C.H. Tsai, C.H. Liao, C.H. Chen, Appl. Phys. Lett. 85 (2004) 3301.
[17] M.F. Lin, L. Wang, W.K. Wong, K.W. Cheah, H.L. Tam, M.T. Lee, C.H. Chen, Appl. Phys. Lett. 89 (2006) 121913.
[18] B.E. Koene, D.E. Loy, M.E. Thompson, Chem. Mater. 10 (1998) 2235.
[19] D.F. O'Brien, P.E. Burrows, S.R. Forrest, B.E. Koene, D.E. Loy, M.E. Thompson, Adv. Mater. 10 (1998) 1108.
[20] M. Watanabe, M. Nishiyama, T. Yamamoto, Y. Koie, Tetrahedron Lett. 41 (2000) 481.
[21] M.J. Plater, T. Jackson, Tetrahedron 59 (2003) 4673.
[22] B. Iorga, F. Eymery, P. Savignac, Tetrahedron 55 (1999) 2671.
[23] A. Suzuki, Pure. Appl. Chem. 57 (1985) 1749.
[24] J.M. Kauffman, G. Moyna, J. Org. Chem. 68 (2003) 839.
[25] A.D. Becke, J. Chem. Phys. 98 (1993) 5648.
[26] C. Lee, W. Yang, R.G. Parr, Phys. Rev. B 37 (1988) 785.
[27] M.J. Frisch, G.W. Trucks, H.B. Schlegel, G.E. Scuseria, M.A. Robb, J.R. Cheeseman, J.A. Montgomery Jr., T. Vreven, K.N. Kudin, J.C. Burant, J.M. Millam, S.S. Iyengar, J. Tomasi, V. Barone, B. Mennucci, M. Cossi, G. Scalmani, N. Rega, G.A. Petersson, H. Nakatsuji, M. Hada, M. Ehara, K. Toyota, R. Fukuda, J. Hasegawa, M. Ishida, T. Nakajima, Y. Honda, O. Kitao, H. Nakai, M. Klene, X. Li, J.E. Knox, H.P. Hratchian, J.B. Cross, C. Adamo, J. Jaramillo, R. Gomperts, R.E. Stratmann, O. Yazyev, A.J. Austin, R. Cammi, C. Pomelli, J.W. Ochterski, P.Y. Ayala, K. Morokuma, G.A. Voth, P. Salvador, J.J. Dannenberg, V.G. Zakrzewski, S. Dapprich, A.D. Daniels, M.C. Strain, O. Farkas, D.K. Malick, A.D. Rabuck, K. Raghavachari, J.B. Foresman, J.V. Ortiz, Q. Cui, A.G. Baboul, S. Clifford, J. Cioslowski, B.B. Stefanov, G. Liu, A. Liashenko, P. Piskorz, I. Komaromi, R.L. Martin, D.J. Fox, T. Keith, M.A. Al-Laham, C.Y. Peng, A. Nanayakkara, M. Challacombe, P.M.W. Gill, B. Johnson, W. Chen, M.W. Wong, C. Gonzalez, J.A. Pople, Gaussian 03, Revision A.1, Gaussian, Inc., Pittsburgh PA, 2003.
[28] L.S. Hung, L.R. Zheng, M.G. Mason, Appl. Phys. Lett. 78 (2001) 673.

[29] Y.S. Wu, T.H. Liu, H.H. Chen, C.H. Chen, Thin Solid Film 496 (2006) 626.
[30] S.A. Van Slyke, C.H. Chen, C.W. Tang, Appl. Phys. Lett. 69 (1996) 2160.
[31] H.J. HainK, J.E. Adams, J.R. Huber, Ber. Bunsenges, Phys. Chem. 78 (1974) 436.
[32] S.N. Frank, A.J. Bard, J. Electrochem. Soc. 122 (1975) 898.